

## Static Friction Coefficient into Cylindrical Joints Assemblies

A. Todi-Eftimie<sup>a</sup>, S. Bobancu<sup>b</sup>, C. Gavrilă<sup>a</sup>, L. Eftimie<sup>c</sup>

<sup>a</sup>Department of Product Design, Mechatronics and Environment, Transylvania University, Brasov, Romania,

<sup>b</sup>Schaeffler Technologies AG & Co. KG, Germany,

<sup>c</sup>Department of Materials Engineering and Welding, Transylvania University, Brasov, Romania.

### Keywords:

Cylindrical joint  
Static friction coefficient  
Dry/lubricated friction  
Bush chain  
Sprocket

### ABSTRACT

The aim of this research is to analyze the behavior of the transition between static and dynamic friction coefficient in a cylindrical joint, in order to reach high reliability when loads are acting. The friction between cylindrical contact faces is analyzed both in dry and lubricated conditions up to the moment that the assembly starts moving while tilting the entire assembly. It means that it is analyzed a complex static friction developed along a chain and its sprocket.

### Corresponding author:

Alina Todi-Eftimie  
Department of Product Design,  
Mechatronics and Environment,  
Transylvania University, Brasov,  
Romania.  
E-mail: [alina.eftimie@unitbv.ro](mailto:alina.eftimie@unitbv.ro)

© 2015 Published by Faculty of Engineering

## 1. INTRODUCTION

As a non-dimensional parameter, the friction coefficient - a highly investigated topic in tribology [1-4] - normally depends on surface roughness, temperature, and relative charge under static effort [5-7]. We cannot establish the fundamental static friction coefficient and we are proceeding only to check the static friction coefficient between chain and sprocket just before the movement starts. Generally, the experiments establish the dynamic friction coefficient and are not certifying the values before the movement starts. This is good enough for practical behavior of the most important

application of industrial use, because the major damages appear during the start of the movement [8]. In some specific applications, especially for the chain - sprocket assembly we recommend to establish experimentally the static friction coefficient, which has a major influence in the assembly wear and reliability [9,10]. The tribological processes involved in static friction coefficient experimental measurement [11], approach a complex technology designed to establish the static friction coefficient value of the metallic couple of materials in order to reach a better reliability for the chain - sprocket assembly.

## 2. EXPERIMENTAL APPARATUS

In order to determine the static friction coefficients, which appear at the limit between the rest and the movement status, we have converted the chain-sprocket assembly contact using the natural rolling sprocket over its chain, acting under gravitational field load. The movement is governed by the vertical load  $G$ , due to gravitational weight decomposed by the angle  $\alpha$  of a tapered plane into  $G_t$  and  $G_n$  components, as shown in Fig. 1. Along the inclined surface acts the static friction force,  $F_f$ . Adjusting the angle of the tapered plane of the tribometer assembly, we can adjust the force  $G_t$  that is acting along the inclined surface, in order to establish the exact moment of movement start and the force that is promoting the exit of the assembly from the immobility status.

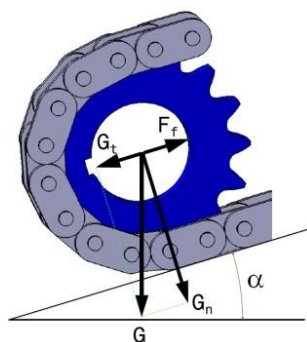


Fig. 1. Static friction coefficient in chain-sprocket assembly.

The simple design of the tribometer [12] presented in Fig. 2, allows easy relocation to act in specific designed environments, while, in the same time, the precise adjustment and basic horizontality accuracy provides precise measurement. It consists of a base plate and a mobile plate, which rotates around a precise cylindrical joint in the lower side of the tribometer (point A). The tilting of the mobile plate is actuated by a screw-nut transmission - inclined with the angle  $\beta = 60^\circ$  relative to the horizontal plane, which lifts the mobile plate using a metallic or glass ball, set at the end of the screw, in direct contact to the mobile plate. All the contact surfaces from the transmissions are smooth grinded and require precise machining. The base plate can be horizontally aligned using specific adjustable supports.

Two clamps are fixing on the mobile plate two identical chain samples into required parallel alignment to the tilting direction, as showed in

Fig. 2, while a mobile pair of sprockets is laid on the chain samples. The two sprockets are fixed at the opposite sides of a shaft, on which different weights can be mounted. The other ends of the chains can be fixed straight and tensioned on the mobile plate with two clamps, or rolled on the sprocket and fixed by the last link to the chain.

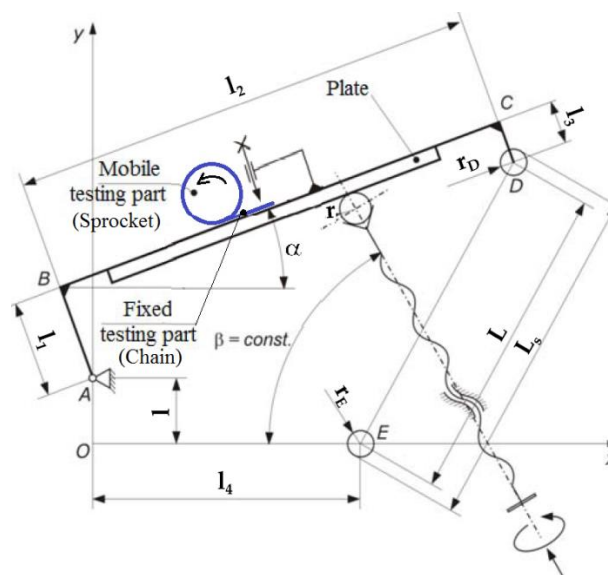


Fig. 2. Functional diagram of tribometer to determine static friction coefficients [13].

After setting the sprockets on the chain samples, the mobile plate is tilted up to the precise moment when the rolling of the sprockets on the chains starts. At this point, the static friction coefficient can be computed by measuring the tilting angle of the mobile plate.

The tilting angle of the mobile plate will be determined by measuring the distance  $L_s$  over a pair of pins fixed on the base plate and the mobile plate. We calculate the tilting angle introducing the measured values into a nonlinear function [13] of type (1):

$$\alpha_1 = \alpha(L_s) \quad (1)$$

In order to achieve a better accuracy and to minimize measuring errors, we have used three pairs of pins - three fixed on the base plate and the other three fixed on the mobile plate. The pins are positioned at specific distances one to each other, such that measuring the three different distances between each pair, we can compute the same angle  $\alpha$ .

Using custom software, in which all the device parameters are constants and the only variables

are the distances  $L_s$ , measured over the pins, the static friction coefficients are computed and presented as a graph or tabular values. Possible errors that can appear during measurements are minimized within the software, which is analyzing many test values. The software is programmed to compare the three measured values of the distance  $L_s$ , to realize different mean values between them, and to choose for each test the final average value of the static friction coefficient for the ones with values closer to each other, in the limits of allowed deviation of 1 %.

### 3. EXPERIMENTAL DETERMINATIONS

Comparative studies referring to various chain - sprocket assembly types, acting in lubricated or acting in dry conditions have been realized. This analysis shows how the general static friction coefficient is managed by the load, which is acting on the chain - sprocket assembly during the moment before movement start. To simulate different usual lubrication conditions, the assembly can be emerged in lubricating oil, or the oil can be sprinkled on the chain surface, before the surfaces get into contact. The tests were realized in conditions of temperature between 25 ... 28 °C, humidity percentage of the atmosphere of 80 %. The tests analyzed into this paper were completed in order to establish the static friction coefficient using lubrication by sprinkling oil on the chain and without primary lubrication. The force (marked with  $G$  in Fig. 1) acting on each sprocket - chain assembly was established at 32 N.

The chains selected for this test were B8 (with a pitch diameter of 8 mm) and B9 (with a pitch diameter of 9.5 mm) bush chains together with their sprockets. The measured values of the static frictional coefficient for both of the B8 and B9 bush chains - sprocket assemblies, without and with lubrication, are presented in Table 1. The medium static friction coefficients for each type of testing were computed as mean values of the testing measurements, excepting the minimum and the maximum values of the series.

From Table 1, we can observe that for the B9 bush chain - sprocket assembly, without lubrication, the static friction coefficient is slightly smaller than for B8 bush chain -

sprocket assembly. It means that the static friction coefficient is depending on the increase of the radiuses of cylindrical joints in contact. In addition, the increased static friction coefficient trend applies for the same B9 bush chain - sprocket assembly, with lubrication.

**Table 1.** Static friction coefficients and wear rates.

B8 chain static friction coefficient comparison		B9 chain static friction coefficient comparison	
B8 without lubrication	B8 with lubrication	B9 without lubrication	B9 with lubrication
0.1323	0.1330	0.1282	0.1286
0.1319	0.1343	0.1275	0.1295
0.1311	0.1352	0.1281	0.1314
0.1322	0.1349	0.1271	0.1297
0.1303	0.1369	0.1251	0.1305
0.1305	0.1336	0.1263	0.1287
0.1315	0.1360	0.1256	0.1295
0.1307	0.1350	0.1265	0.1304
0.1314	0.1358	0.1256	0.1298
0.1312	0.1339	0.1254	0.1289
0.1302	0.1346	0.1261	0.1294
0.1303	0.1342	0.1254	0.1297
μ med.*			
0.1311	0.1348	0.1264	0.1296
% difference			
0%	2.78%	0%	2.57%

\* medium values computed for the measured values, excepting the minimum and maximum values of the series.

Comparing both the B8 and B9 bush chain - sprocket assemblies, we can observe an increase of the static friction coefficient of 2.78 %, respectively 2.57 %. This means that in the cylindrical joints in contact, the phenomenon of adhesion due to superficial stress into the lubricant oil film appears [14,15].

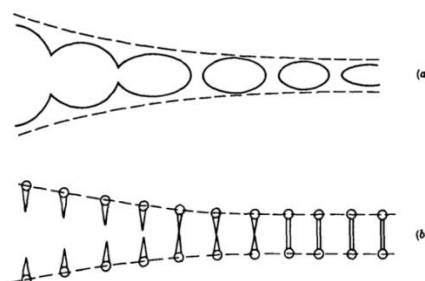


**Fig. 3.** Cumulative dilatational fractures between two lubricated couple of materials [16] by a) growth and coalescence of holes through viscous or plastic flow; b) stretching and rupture of atomic bonds.

Adhesion is the tendency of dissimilar particles or surfaces to cling to one another (Fig. 3). The

real area of contact between two surfaces is only a small fraction of the apparent area of contact. This means that even with quite small loads, very large pressures will be developed into the few points of real contact. These pressures are sufficient to cause local adhesion and welding of the surfaces into the singular points of contact. The tangential force required to shear the junctions is a major component of the friction between sliding metal surfaces [17-22].

Taking into consideration the contact configuration of the cylindrical joint between a bush chain and its sprocket, we can accept that the contact of the parallel axes is linear. According to Hertzian theory, under the action of a distributed pressure  $P$ , normal to the contact line, as showed in Figs. 4a) and 4b), the line is transforming into an elliptical cross section cylinder of length  $L$  and width  $b$ .

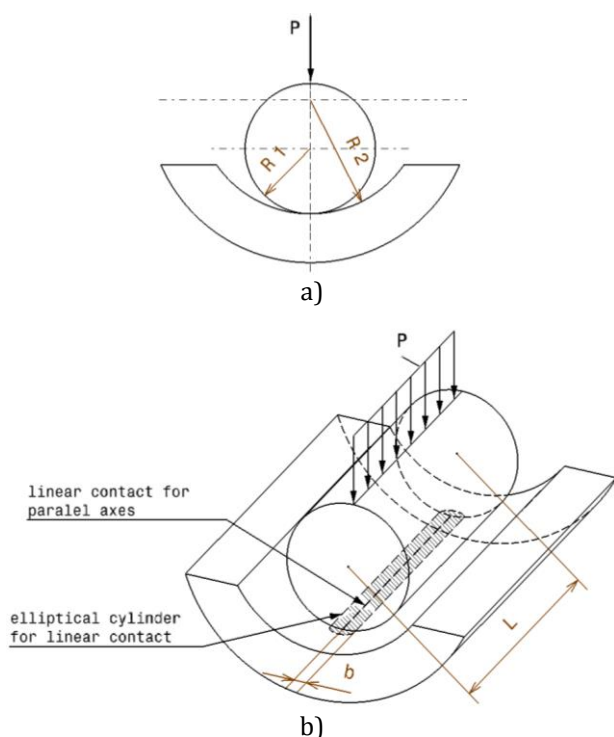


**Fig. 4.** Linear cylindrical joint contact with parallel axes: a) front view; b) isometric view.

In the graphic from Fig. 5 are presented the measured static friction coefficients for a B8 bush chain tested without lubrication and with lubrication. We have established that for the static friction coefficient of the B8 bush chain-sprocket assembly, tested without lubricant, the resulted values are in the range of 0.1311. The slightly increase of the measured values for the tests of the chain with lubrication, compared to

the tests without lubrication, maintains a small dispersion of the values, around 0.1348. A repetitive set of measurements have been realized, in order to validate the achieved experimental data.

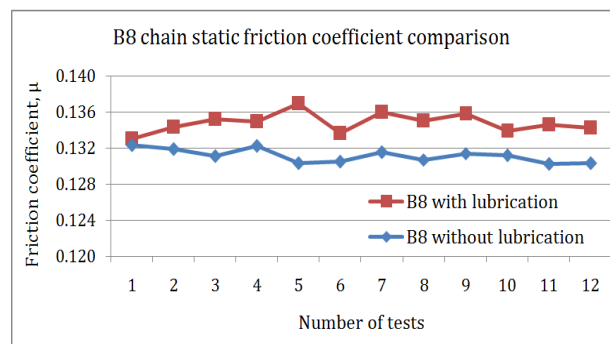


**Fig. 5.** Static friction coefficients for B8 bush chain with lubrication vs. B8 bush chain without lubrication.

The graphic from figure 6 presents measured static friction coefficients for a B9 bush chain tested in two different environment: without lubrication and with lubrication. During tests, the measured values maintain the same trend as for the B8 bush chain, but the values are somewhat decreased. For the static friction coefficient of the B9 bush chain-sprocket assembly, tested without lubricant, the resulted values are in the range of 0.1264. There is also a slightly increase of the measured values for the tests of the chain with lubrication compared to the tests without lubrication. The measured values maintain a small dispersion of the values, around 0.1296. This concludes that the repetitive measurements have been accurate and the experimental data is valid.

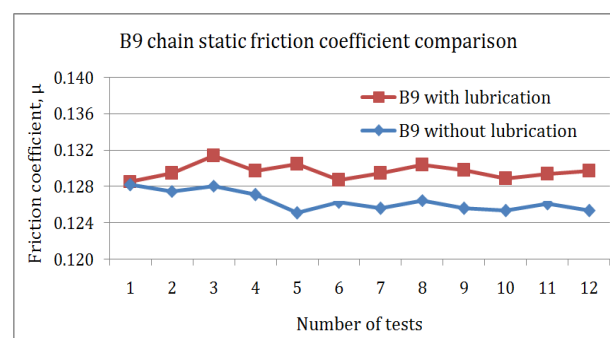


**Fig. 6.** Static friction coefficients for B9 bush chain with lubrication vs. B9 bush chain without lubrication.

In both graphics from Figs. 5 and 6, the initial values of the testing series for the chains with lubricant tend to approach, but they are distancing as the lubricant film fills all the contact areas.

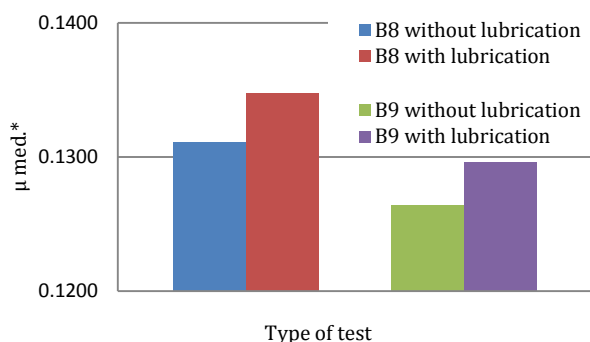


**Fig. 7.** Medium static friction coefficients comparison.

The comparison from the graphic in Fig. 7 shows an overview of the tested chain dimensions, under conditions of testing with lubrication and without lubrication. The static friction coefficient for the B8 bush chain has bigger values for both testing conditions of lubrication, comparing to the B9 bush chain. As seen in Fig. 7, both B8 and B9 bush chains obtained bigger static friction coefficients for tests realized with lubrication, than for the tests without lubrication.

#### 4. CONCLUSIONS

As a non-dimensional parameter, the friction coefficient normally depends on surface roughness, temperature, and relative charge under static effort on the surfaces in contact. Because we cannot measure the fundamental pure static friction coefficient, we are proceeding to check the static friction coefficient between chain and sprocket just before the movement starts. The experiments are establishing not the dynamic friction coefficient and are not certifying the values before the movement starts. The necessity of this analysis is due to the major damages that appear in the chain - sprocket assembly during the start of the movement. For the specific applications, as the chain - sprocket assembly, the experimentally measurement values of the static to dynamic limit of friction coefficient can be appreciated as a major governor of the assembly wear and reliability.

The tribological process analysis is applied to the transition between static and dynamic friction and is based on experimental measurement, approaching a complex measurement technology, in order to increase the chain - sprocket reliability.

The experiments and the analyses based on this new approach to the physic's phenomena establish a real measured limit of the static to dynamic friction coefficient value for the couple of materials.

#### REFERENCES

- [1] B. Jeremic, D. Vukelic, et al., 'Static Friction at High Contact Temperatures and Low Contact Pressure', *Journal of Friction and Wear*, vol. 34, no. 2, pp. 114-119, 2013.
- [2] A. Gummer and B. Sauer, 'Influence of Contact Geometry on Local Friction Energy and Stiffness of Revolute Joints', *ASME Journal of Tribology*, vol. 134, no. 2, pp. 9, 2012.
- [3] V. Mortazavi, C. Wang and M. Nosonovsky, 'Stability of Frictional Sliding With the Coefficient of Friction Depended on the Temperature', *ASME Journal of Tribology*, vol. 134, no. 4, pp. 7, 2011.
- [4] J.M. Garcia and A. Martini, 'Measured and Predicted Static Friction for Real Rough Surfaces in Point Contact', *ASME Journal of Tribology*, vol. 134, no. 3, pp. 8, 2012.
- [5] C.A. Pereira, J. Abrosio and A. Ramalho, 'Influence of contact modeling on the dynamics of chain drives', in *The IV-th European Conference on Computational Mechanics*, Paris, France, 2010.
- [6] S. Pedersen, 'Model of contact between rollers and sprockets in chain-drive systems', *Archive of Applied Mechanics*, vol. 74, pp. 489-508, 2005.
- [7] S. Metil'kov, S.B. Bereznoi and V.V. Yunin, 'Wear of hinges in roller drive chain', *Russian Engineering Research*, vol. 28, no. 9, pp. 839-844, 2008.
- [8] C. Jaliu, A.L. Todi-Eftimie and R. Saulescu, 'Solutions to optimize transmission chains characteristics', *Proceedings of the Annual Session of Scientific Papers "IMT Oradea - 2012"*, vol. XI (XXI), no. 2, 2012.
- [9] A.L. Todi-Eftimie and L. Eftimie, 'Influence of the contact sliding surface shape on wear development during reciprocating movement', *Metalurgia International (ISI)*, vol. 18, no. 5, p. 159, 2013.
- [10] A. Todi-Eftimie, R. Velicu, R. Saulescu and C. Jaliu, 'Geometric modeling of power joints from bush chain drives', *The 11-th IFToMM Intl. Symposium of Science of Mechanisms and Machines*, vol. 18, pp. 471-479, 2013.

- [11] V.I. Bakhshaliev, 'The problem of mathematical simulation of rolling friction', *Journal of Friction and Wear*, vol. 30, no. 5, pp. 305-308, 2009.
- [12] Ș. Bobancu, Certificat de inovator Nr. 25 din 14.06.2004.
- [13] R. Cozma, 'Contribuții la studiul frecării în mișcarea de translație prin realizarea și experimentarea unei categorii de aparate de înaltă precizie', *Teză de doctorat*, Brașov, 1995.
- [14] J.B. Adams, L.G. Hector, et al., 'Adhesion, lubrication and wear on the atomic scale', *Surface And Interface Analysis*, vol. 31, no. 7, pp. 619-626, 2001.
- [15] S. Hao and L.M. Keer, 'Rolling Contact Between Rigid Cylinder and Semi-Infinite Elastic Body With Sliding and Adhesion', *ASME Journal of Tribology*, vol. 129, no. 3, pp. 14, 2007.
- [16] D. Buckley, *Surface effects in adhesion, friction, wear, and lubrication*. Netherlands: Elsevier Scientific Publishing Co., 1981.
- [17] F.P. Bowden and A.J.W. Moore, 'Adhesion of Lubricated Metals', *Nature*, vol. 155, pp. 451-452, 1945.
- [18] A. Faghihnejad and H. Zeng, *Fundamentals of Surface Adhesion, Friction, and Lubrication. Polymer Adhesion, Friction, and Lubrication*. Ed. John Wiley & Sons, Inc., Hoboken, USA, 2013.
- [19] H. Zeng, *Polymer Adhesion, Friction, and Lubrication*. Ed. John Wiley & Sons, 2013.
- [20] M.D. Pascovici and T. Cicone, *Elemente de tribologie*. Ed. Bren, Bucuresti, 2001.
- [21] C. Pereira, A. Ramalho and J. Abrosio, 'Verification process of cylindrical contact force models for internal contact modeling', *World Academy of Science, Engineering and Technology*, vol. 77, pp. 250-260, 2013.
- [22] J.P. Shi, K. Ma and Z.Q. Liu, 'Normal Contact Stiffness on Unit Area of a Mechanical Joint Surface Considering Perfectly Elastic Elliptical Asperities', *ASME Journal of Tribology*, vol. 134, no. 3, pp. 6, 2012.